IEEE Access
Multidisciplinary | Rapid Review | Open Access Journal

Received April 13, 2020, accepted April 26, 2020, date of publication April 30, 2020, date of current version May 13, 2020.

Digital Object Identifier 10.1109/ACCESS.2020.2991551

A Dual-Cavity Fabry–Perot Interferometric Fiber-Optic Sensor for the Simultaneous Measurement of High-Temperature and High-Gas-Pressure

YANG CUI[1], YI JIANG[1], TIANMU LIU[1], JIE HU[2], AND LAN JIANG[2]
[1]School of Optics and Photonics, Beijing Institute of Technology, Beijing 100081, China
[2]Laser Micro/Nano Fabrication Laboratory, School of Mechanical Engineering, Beijing Institute of Technology, Beijing 100081, China

Corresponding author: Yi Jiang (bitjy@bit.edu.cn)

This work was supported in part by the National Key Research and Development Program of China under Grant 2018YFB1107200, in part by the National Natural Science Foundation of China (NSFC) under Grant 61775020, and in part by the Program of Chinese 863 Project under Grant 2015AA043504.

ABSTRACT A fiber optic dual-cavity Fabry–Perot interferometer(DFPI) for simultaneous high- temperature and high-gas-pressure measurements is proposed and experimentally demonstrated. The proposed sensing structure consists of an extrinsic Fabry–Perot interferometer (EFPI) with a short piece of hollow core fiber (HCF) for gas pressure sensing, and an intrinsic Fabry–Perot interferometer (IFPI) made of photonic crystal fiber (PCF) for temperature sensing. The composite interference signal is filtered in the frequency domain to obtain two independent interference spectra, and then is demodulated by using white light interferometry (WLI). The experimental results show that the sensor exhibits good linearity over a temperature range from 40 to 1000°C with a cavity-length temperature sensitivity of 25.3 nm/°C, and a pressure range from 0 to 10 MPa with a cavity-length pressure sensitivity of 1460 nm/MPa at 40°C. This proposed sensor are light-weight and small, and it has a compact structure and a high temperature resistance.

INDEX TERMS Optical fiber sensors, Fabry-Perot, temperature measurement, pressure measurement.

I. INTRODUCTION

In recent years, there has been an urgent demand for temperature and pressure measurements in the high-temperature and high-gas-pressure environments of turbine engines, high-speed aircraft, and other aerospace applications. At present, the existing electrical sensors cannot operate in extreme environments. Optical fiber sensors have the advantages of high temperature resistance, electromagnetic interference immunity, small volumes and passive sensing, making them suitable for measuring temperatures and gas pressures in some extreme environments. Initially, fiber Bragg gratings (FBGs) were widely used for hybrid measurements of temperature and pressure. A FBG is fabricated by periodically changing the refractive index of the core with ultraviolet light and fiber-core doped Ge. Thus, a FBG cannot work over 300°C for a long time [1]–[4]. Subsequently, IFPIs and EFPIs have gradually played increasing roles in high-temperature and high-pressure measurements due to their high temperature resistance and high sensitivity. In general, an IFPI is used for temperature measurements [5], [6], and an EFPI is used for pressure measurements [7], [8]. To simultaneously measure the temperature and gas pressure, it is necessary to combine two types of interferometers. The most common type of such a sensor is a DFPI, which is a temperature-pressure composite sensor [9], [10]. Generally, there are two ways for EFPIs to measure pressure, including the diaphragm type [11], and diaphragm-free type [12]. A femtosecond laser was employed to ablate a film at the end of a fiber and form a pressure sensor with a measurement range of 0-0.7 MPa, and a cascaded IFPI achieved a large temperature measurement range of 20-700°C [13]. However, for diaphragm pressure sensors in high-temperature environments with the temperatures greater than 800°C, the diaphragm will creep, resulting in measurement errors, and it will not return to the initial state after the temperature drops. Therefore, a diaphragm-free pressure

The associate editor coordinating the review of this manuscript and approving it for publication was Zinan Wang.

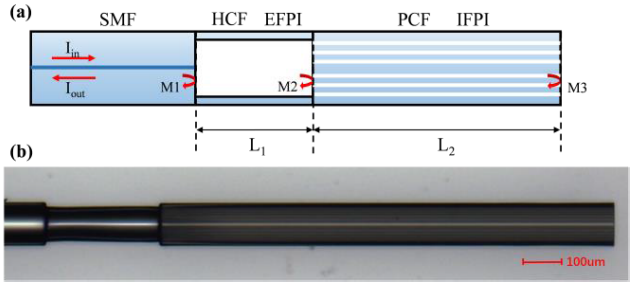

FIGURE 1. (a) Schematic diagram of the DFPI sensor and (b) the microphotograph of the fabricated sensor.

sensor is typically used by measuring the variation in the refractive index (RI) of air at high temperatures. A DFPI fiber sensor, which achieves a wide range of simultaneous temperature and pressure measurements with a measurement range of 0-10 MPa at 40-1100°C, was demonstrated in a previous study [14]. In addition, in terms of the fabrication process, the previously reported DFPI hybrid structures, which use either chemical etching [15] or laser micromachining [11], require a complicated series of steps or expensive equipment.

In this paper, a DFPI fiber-optic sensor is proposed and demonstrated for the simultaneous measurement of gas pressures and temperatures over a wide pressure range of 0–10 MPa and a wide temperature range of 40–1000°C. The sensor is formed by sequentially splicing a single mode fiber (SMF), a hollow core fiber (HCF) and a photonic crystal fiber (PCF) via a fabrication process that is simple and mature. The interference signal is demodulated by using a fast Fourier transform (FFT) and a white light interferometry (WLI) demodulation algorithm. The sensor adopts an all-fiber structure and exhibits high sensitivity and stability over wide temperature and pressure measurement ranges.

II. DESIGN AND CALCULATION

The proposed DFPI-based high-temperature and high-gas-pressure sensor consists of a SMF, HCF, and PCF, as shown in Fig. 1(a). The EFPI is made of a HCF with an inner diameter of 93 μm and an outer diameter of 125 μm. The IFPI is made of a PCF with a solid center and a hexagonal hole array with a diameter of 85 μm. To avoid the air holes of the PCF from being blocked by the thick wall of the HCF, the inner diameter of the HCF should be larger than the diameter of the hexagonal hole array of the PCF. The production process is divided into two steps. First, we spliced the SMF and the HCF and then cleaved the HCF at a distance of L_1 from the splicing point. Second, a PCF was spliced with the HCF, and we then cleaved the PCF at a distance of L_2 after the splicing point. The fabricated sensor is shown in Fig. 1(b).

When broadband light is injected into the lead-in SMF, it will generate the first reflection at the splice point of the SMF and HCF, denoted as M1. After the transmitted light passes through the HCF, a second reflection occurs at the splice point of the HCF and the PCF, denoted as M2. Then, the transmitted light enters the PCF and generates a third reflection at the end face of the PCF, denoted as M3. The reflection beams form three-beam interference that is measured by a manually constructed WLI demodulator. The composite interference spectrum is processed by a FFT. Two bandpass filters with different center frequencies are used to filter out the frequency of interest. We can obtain the separate interference spectrum of the corresponding frequency by an inverse fast Fourier transform (IFFT). Then, the optical path difference corresponding to each interference spectrum can be obtained by the WLI demodulation algorithm [16].

Temperature measurements are realized by measuring the thermo-optic effect and thermal expansion of the IFPI, and the pressure measurements are obtained by measuring the refractive index change in the air in the EFPI. The refractive index of air is sensitive to the pressure. The optical path differences of the EFPI and IFPI, OPD_1 and OPD_2, are as follows:

$$OPD_1 = 2n_1L_1 \tag{1}$$

$$OPD_2 = 2n_2L_2 \tag{2}$$

where n_1 is the refractive index of air, n_2 is the refractive index of the PCF, L_1 is the length of the EFPI cavity, and L_2 is the length of the IFPI cavity.

The principle of the pressure measurement is that the pressure changes the refractive index of the air. According to Eq.1, the change in the refractive index n_1 of the EFPI cavity is the change in the optical path difference of the EFPI (OPD_1). The refractive index n_1 is affected by the pressure P, temperature T and air, which can be expressed as [17]:

$$n_1 = 1 + \frac{a \times P}{1 + b \times T} \tag{3}$$

where a (/Pa) and b (/°C) are coefficients that are affected by the air. In this experiment, standard atmosphere (dry air, 101.325 kPa) is used. Additionally, $a = 2.9 \times 10^{-9}$/Pa, and $b = 3.7 \times 10^{-3}$/°C [15]. The pressure sensitivity of the EFPI, S_P (μm/Pa), is expressed as:

$$S_P = \frac{dOPD_1}{dP} = \frac{dn_1}{dP}2L_1 = \frac{a \times 2L_1}{1 + b \times T} \tag{4}$$

The principle of the temperature measurement is based on the thermo-optic effect and the thermal expansion effect of the PCF. According to Eq. 2, the expression of the temperature sensitivity S_T (μm/°C) is:

$$S_T\frac{dOPD_2}{dP} = (\frac{1}{n}\frac{dn_2}{dT} + \frac{1}{L_2}\frac{dL_2}{dT})OPD_2 = (\varepsilon + \alpha)OPD_2 \tag{5}$$

where ε ($\varepsilon = 8.3 \times 10^{-6}$/°C) is the thermo-optic coefficient, α ($\alpha = 0.55 \times 10^{-6}$/°C) is the thermal expansion coefficient, and $n_2 = 1.44$. According to the initial temperature T_0 and the optical path difference variation ΔOPD_2, the corresponding temperature T can be obtained:

$$T = \frac{1}{(\varepsilon + \alpha)OPD_2}\Delta OPD_2 + T_0 \tag{6}$$

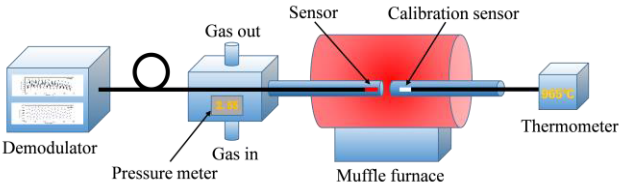

FIGURE 2. The experimental setup.

Since the EFPI cavity is affected by the temperature and pressure, we can calculate the temperature T in real time through the IFPI cavity and apply this value to determine the pressure sensitivity S_P of the EFPI. The pressure measurement value P after temperature compensation can be described as follows.

$$P = \frac{1 + b \times T}{\alpha \times 2L_1} \Delta OPD_1 + P_0 \tag{7}$$

where P_0 is the initial pressure. In standard atmosphere, $P_0 = 0$ is generally considered.

In this paper, L_1 is selected as 307.5 μm and L_2 is 1263.2 μm, that is OPD_1 and OPD_2 are 615 μm and 3638 μm, respectively. The first reason for these values is that the frequencies of the EFPI and IFPI have obvious differences during the filtering process. The second reason is that the number of periods should be maximized in a spectral range of 80 nm, which is convenient for subsequent calculations. When $L_1$and L_2 are substituted into Eq.4 and Eq.5, the theoretical temperature sensitivity is 25.5 μm /°C, and the theoretical pressure sensitivities are 1485.2 nm/MPa at 40°C and 383.2 nm/MPa at 1000°C.

III. EXPERIMMENTS AND RESULTS

The high-temperature and high-gas-pressure measurement system is shown in Fig. 2. The fiber optic sensor is inserted into a ceramic tube. The ceramic tube is connected to the pressure meter for pressurized air. The entire system is sealed, ensuring a stable pressure during the pressure measurement process. The measurement resolution of the pressure meter is 0.01 MPa. Then, the ceramic tube with the sensor is placed in the central constant temperature zone of a muffle furnace (GHA 12/300, Carbolite) for the temperature measurement. The demodulator is a manually constructed WLI demodulator. The FP cavity demodulation resolution is 1 nm when the optical path difference is less than 1 mm. The measurement frequency is 1Hz. In this article the temperature and pressure measurements are quasi-static processes, so the measurement frequency of 1 Hz can reflect its changes.

The demodulation process of the demodulator is shown in Fig. 3. First, the interference signal diagram of the DFPI sensor is acquired as shown in Fig. 3(a). After FFT, the frequency domain signal is shown in Fig. 3(b). There are three peaks in the frequency domain signal. Peaks1, 2 and 3 represent the EFPI, IFPI, and large FP cavity formed by the EFPI and IFPI, respectively. We select two bandpass filters with center frequencies at peak 1 and peak 2 to filter the two signals separately. To facilitate the subsequent

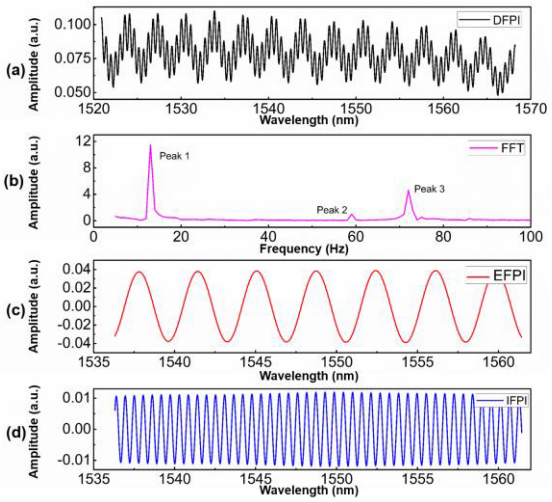

FIGURE 3. (a) The spectrum of the back reflected light, (b) the FFT spectrum of the DFPI sensor, and the recovered spectra of the (c) EFPI and the (d) IFPI.

calculation of the OPD, we appropriately intercepted the filtered spectrum, that is, only a part of the spectrum is selected for the calculation within the chosen range of 1535-1565 nm. The EFPI interference spectrum in Fig. 3(c) and IFPI interference spectrum in Fig. 3(d) are obtained by performing IFFT. Two interference spectra are obtained separately to calculate the values of OPD_1 and OPD_2 with the WLI demodulation algorithm. For this sensor, OPD_1 is 615 μm and OPD_2 is 3638 μm at room temperature and standard atmospheric pressure.

The temperature and the pressure responses of the sensor were investigated. First, the sensor was aged by heating the muffle furnace at 1000°C for one hour to remove the residual stress of the sensor. Then, the furnace was naturally cooled to room temperature. The muffle furnace was heated from 40°C to 1000°C at a step of 100°C. To maintain a stable and consistent temperature in the muffle furnace, the temperature was maintained for one hour at each temperature point. From Fig. 4, we can see that the temperature response is linear and that the corresponding sensitivity is 25.3 μm/°C (R^2 =0.99653), which deviates from the theoretical value of 25.5 μm/°C by 0.2 μm/°C.

According to the linear relationship between OPD_2 and the temperature, we measured the actual temperature value. A comparison between the calibration value and the measured value is shown in Fig. 5. The measured value is close to the calibration value, and the maximum error is less than 3% over the full scale of values.

When the temperature was stable at each heating step, the pressure response was investigated. A pressurization process with a step of 1 MPa in the range of 0-10 MPa was implemented. The measured pressure data at each temperatures point are as shown in Fig. 6. Fig. 7 shows that the pressure sensitivity decreases with increasing temperature, and the measured value is in agreement with the theoretical

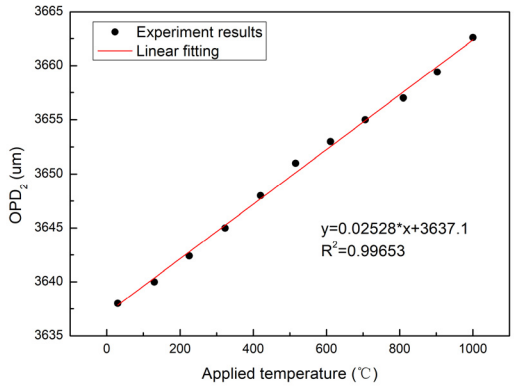

FIGURE 4. The relationship between OPD_2 and the applied temperature.

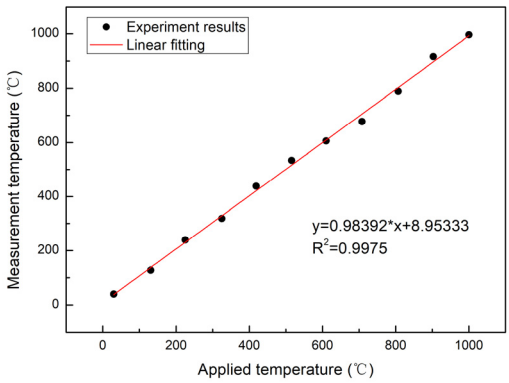

FIGURE 5. Temperature measurement results.

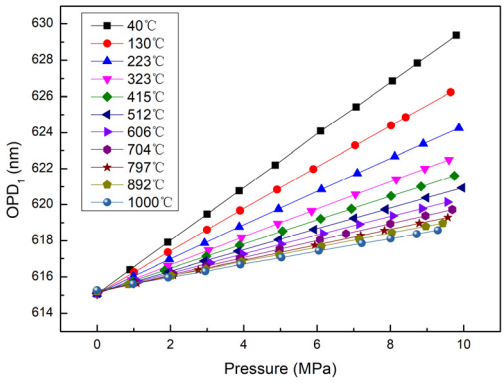

FIGURE 6. The relationship between OPD_2 and the applied pressure.

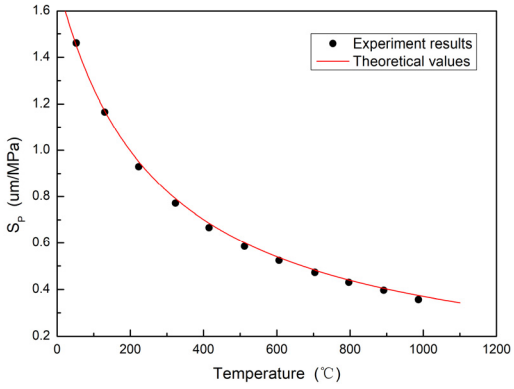

FIGURE 7. The relationship between the pressure sensitivity and the temperature.

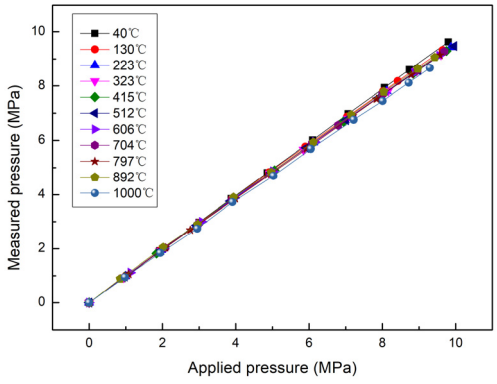

FIGURE 8. Pressure measurement results at different temperatures.

value. In the temperature range of 40-1000°C, the pressure sensitivity changes by 1103.5 nm/MPa. The pressure sensitivity is 1460 nm/MPa at 40°C and 356.5 nm/MPa at 1000°C. The measured value and theoretical values of pressure sensitivity are different due to temperature measurement errors. In addition, the initial length of the EFPI is influenced by the temperature. From 40°C to 1000°C, the length of the EFPI changed from 615.05 μm to 615.25 μm. This influence can be ignored for the pressure measurements.

The pressure measurements are affected by the temperature T according to Eq.7. Therefore, we need to obtain the temperature in real time while measuring the pressure. We can adopt the temperature value estimated by the temperature sensor IFPI in Eq.4. Thus the sensitivity at the corresponding temperature can be obtained. The pressure value can be determined according to Eq.7. And the influence of the temperature on the pressure measurement can be removed. The measured values and calibration data are shown in Fig. 8. Fig. 9 shows the error bar, which is the percentage of the difference between the measured pressure and the standard pressure at each standard pressure in the range of 0-10 MPa.

Fig 8 shows that the pressure measurements within a range of 0-10 MPa display a good linear relationship with the temperature range of 40-1000°C. The accuracy of the pressure measurements in the low-temperature range is high, while there is a deviation at high temperatures. Fig. 9 shows that the error increases with increasing pressure over the entire temperature range. Near temperatures of approximately 900°C, the error at each pressure gradient position does not exceed 5% of the full scale. The reason may be that the temperature measured by the IFPI becomes less accurate as the temperature increases, which causes an error in the temperature compensation of the pressure sensor, and leads to pressure measurement error. However, at 1000°C, the error increases

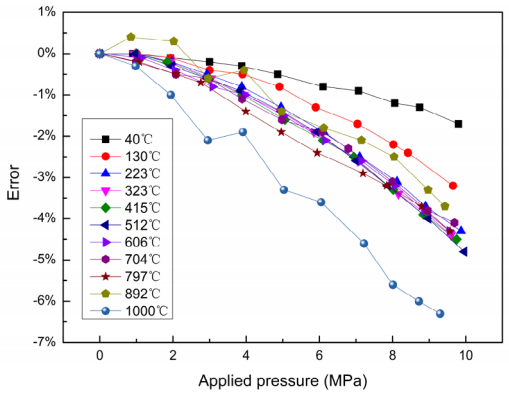

FIGURE 9. Measurement error.

significantly, reaching 7%. The main reason is that the optical fiber material is quartz, the sensor is softened at 1000 °C and the sensor performance is reduced. Therefore the sensor cannot be used at 1000 °C for a long time.

IV. CONCLUSION

In summary, a dual-cavity fiber optic sensor for simultaneous temperature and gas pressure measurements in extreme environments is proposed and experimentally demonstrated. The sensor structure is an EFPI made of HCF cascaded with an IFPI made of PCF. The cavity lengths of the EFPI and IFPI are 307.5 μm and 1263.2 μm, respectively. The interference spectrum is demodulated by FFT and the WLI demodulation algorithm. Gas pressures over a range of 0–10 MPa and temperatures over a range of 40–1000°C are measured simultaneously. The experimental results show that the temperature measurement sensitivity is 25.3 μm/°C and the pressure sensitivity is 1460 nm/MPa at 40°C. The pressure sensitivity is affected by temperature. The pressure measurement exhibits high linearity after temperature compensation. The proposed sensor has the merits of a small size, simple structure, low cost, simple fabrication process, excellent linearity, and large dynamic range. It is believed that this sensor will have potential applications in high-temperature environments.

REFERENCES

[1] A. Sun, "Study of simultaneous measurement of temperature and pressure using double fiber Bragg gratings with polymer package," *Opt. Eng.*, vol. 44, no. 3, Mar. 2005, Art. no. 034402.
[2] Y. Liu, Z. Guo, Y. Zhang, K. S. Chiang, and X. Dong, "Simultaneous pressure and temperature measurement with polymer-coated fibre Bragg grating," *Electron. Lett.*, vol. 36, no. 6, pp. 564–566, 2000.
[3] E. Chmielewska, W. Urbańczyk, and W. J. Bock, "Measurement of pressure and temperature sensitivities of a Bragg grating imprinted in a highly birefringent side-hole fiber," *Appl. Opt.*, vol. 42, no. 31, p. 6284, Nov. 2003.
[4] T. Guo, X. Qiao, Z. Jia, Q. Zhao, and X. Dong, "Simultaneous measurement of temperature and pressure by a single fiber Bragg grating with a broadened reflection spectrum," *Appl. Opt.*, vol. 45, no. 13, p. 2935, May 2006.
[5] H. Y. Choi, K. S. Park, S. J. Park, U.-C. Paek, B. H. Lee, and E. S. Choi, "Miniature fiber-optic high temperature sensor based on a hybrid structured Fabry–Pérot interferometer," *Opt. Lett.*, vol. 33, no. 21, pp. 2455–2457, 2008.
[6] E. Li, X. Wang, and C. Zhang, "Fiber-optic temperature sensor based on interference of selective higher-order modes," *Appl. Phys. Lett.*, vol. 89, no. 9, Aug. 2006, Art. no. 091119.
[7] K. Bremer, E. Lewis, B. Moss, G. Leen, S. Lochmann, and I. Mueller, "Conception and preliminary evaluation of an optical fibre sensor for simultaneous measurement of pressure and temperature," in *Proc. J. Phys., Conf. Ser.*, vol. 178, Jul. 2009, Art. no. 012016.
[8] S. H. Aref, H. Latifi, M. I. Zibaii, and M. Afshari, "Fiber optic Fabry–Pérot pressure sensor with low sensitivity to temperature changes for downhole application," *Opt. Commun.*, vol. 269, no. 2, pp. 322–330, 2007.
[9] Y. L. Wang, C. H. Yang, H. C. Jan, G. R. Lin, J. C. Mau, M. Y. Fu, and W. F. Liu, "Simultaneous temperature and pressure measurement using a packaged FBG and LPG," in *Proc. 15th IEEE OECC*, Sapporo, Japan, Jul. 2010, pp. 814–815.
[10] Q. Wang, L. Zhang, C. Sun, and Q. Yu, "Multiplexed fiber-optic pressure and temperature sensor system for down-hole measurement," *IEEE Sensors J.*, vol. 8, no. 11, pp. 1879–1883, Nov. 2008.
[11] S. Ghildiyal, P. Ranjan, S. Mishra, R. Balasubramaniam, and J. John, "Fabry–Pérot interferometer-based absolute pressure sensor with stainless steel diaphragm," *IEEE Sensors J.*, vol. 19, no. 15, pp. 6093–6101, Aug. 2019, doi: 10.1109/jsen.2019.2909097.
[12] H. Liang, P. Jia, J. Liu, G. Fang, Z. Li, Y. Hong, T. Liang, and J. Xiong, "Diaphragm-free fiber-optic Fabry–Pérot interferometric gas pressure sensor for high temperature application," *Sensors*, vol. 18, no. 4, p. 1011, 2018.
[13] Y. Zhang, J. Huang, X. Lan, L. Yuan, and H. Xiao, "Simultaneous measurement of temperature and pressure with cascaded extrinsic Fabry–Pérot interferometer and intrinsic Fabry–Pérot interferometer sensors," *Opt. Eng.*, vol. 53, no. 6, 2014, Art. no. 067101.
[14] L. Zhang, Y. Jiang, H. Gao, J. Jia, Y. Cui, S. Wang, and J. Hu, "Simultaneous measurements of temperature and pressure with a dual-cavity Fabry–Pérot sensor," *IEEE Photon. Technol. Lett.*, vol. 31, no. 1, pp. 106–109, Jan. 1, 2019.
[15] S. Pevec and D. Donlagic, "Miniature all-fiber Fabry–Pérot sensor for simultaneous measurement of pressure and temperature," *Appl. Opt.*, vol. 51, no. 19, pp. 4536–4541, Jul. 2012.
[16] Y. Jiang, "Fourier transform white-light interferometry for the measurement of fiber-optic extrinsic Fabry–Pérot interferometric sensors," *IEEE Photon. Technol. Lett.*, vol. 20, no. 2, pp. 75–77, Jan. 15, 2008.
[17] B. Xu, Y. Liu, D. Wang, D. Jia, and C. Jiang, "Optical fiber Fabry–Pérot interferometer based on an air cavity for gas pressure sensing," *IEEE Photon. J.*, vol. 9, no. 2, Apr. 2017, Art. no. 7102309.

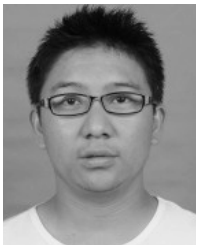

YANG CUI is currently pursuing the Ph.D. degree with the School of Optics and Photonics, Beijing Institute of Technology, China. He has coauthored six publications. His current research interests include sapphire fiber optic sensor and demodulation arithmetic.

YI JIANG received the B.A. and Ph.D. degrees from Chongqing University, Chongqing, China, in 1987. He is currently a Professor with the School of Opto-Electronics, Beijing Institute of Technology, Beijing, China. His research interests include fiber optical sensors, smart structures, and measurement instruments.

TIANMU LIU is currently pursuing the master's degree with the School of Optics and Photonics, Beijing Institute of Technology, China. He is taking in the project sponsored by the National Natural Science Foundation of China. His current research interests include Sapphire fiber sensor and photonic crystal fiber sensor.

JIE HU received the Ph.D. degree from the University of Illinois at Urbana–Champaign, in 2011. She is currently a Professor with the Laser Micro/Nano Fabrication Laboratory, School of Mechanical Engineering, Beijing Institute of Technology. Her research interests include micro-nano machining and micro-nano electrochemical growth.

LAN JIANG received the Ph.D. degree from the Beijing Institute of Technology, Beijing, China, in 2001. He is currently a Professor with the Laser Micro/Nano Fabrication Laboratory, School of Mechanical Engineering, Beijing Institute of Technology. His research interests include optical fiber sensors, surface enhanced Raman scattering, and micromachining.